

Structural Transitions upon Ligand Binding in a Cooperative Dimeric Hemoglobin

WILLIAM E. ROYER, JR.,* WAYNE A. HENDRICKSON,
EMILIA CHIANCONE

Comparison of the 2.4 angstrom resolution crystal structures of dimeric clam hemoglobin in the deoxygenated and carbon-monoxide liganded states shows how radically different the structural basis for cooperative oxygen binding is from that operative in mammalian hemoglobins. Heme groups are in direct communication across a novel subunit interface formed by the E and F helices. The conformational changes at this interface that accompany ligand binding are more dramatic at a tertiary level but more subtle at a quaternary level than those in mammalian hemoglobins. These findings suggest a cooperative mechanism that links ligation at one subunit with potentiation of affinity at the second subunit.

THE EFFICIENCY OF PROTEIN FUNCTION is often improved by having individual functional units act in concert rather than independently of each other. Examples of cooperative functioning of protomers include enzymes and gene-regulating proteins (1). Possibly the most widely studied example of a cooperative allosteric molecule is the mammalian hemoglobin tetramer (2). Cooperative oxygen binding in hemoglobins can be defined as the increase in affinity of the molecule for oxygen as oxygen binding proceeds. A simpler model system for studying cooperative protein function can be found in the hemoglobins of a number of arid blood clams (3). Typically, the dimeric component binds oxygen with constant oxygen affinity over the pH range 5 to 9 and significant cooperativity with a Hill coefficient of 1.5 and a free energy of interaction of about 1 kilocalorie per mole per site (4). The low-resolution structures of the dimeric and tetrameric hemoglobins from *Scapharca inaequalvis* demonstrated the very different quaternary structure of these molecules from mammalian hemoglobins despite the similarity in tertiary structure of the globin chains (5). We reported the 2.4 Å resolution crystal structure of the dimeric hemoglobin in the carbon monoxide (CO)-liganded state (6)

W. E. Royer, Jr., and W. A. Hendrickson, Howard Hughes Medical Institute, Department of Biochemistry and Molecular Biophysics, Columbia University, New York, NY 10032.

E. Chiancone, CNR Center of Molecular Biology, Department of Biochemical Sciences, University 'La Sapienza' 00185 Rome, Italy.

*Present address: Program in Molecular Medicine, University of Massachusetts Medical School, Worcester, MA 01605.

and have now determined the crystal structure, also at 2.4 Å resolution, of the molecule in the deoxygenated (deoxy) state. The comparison of these two structures reveals structural transitions that accompany ligand binding in this cooperative dimer.

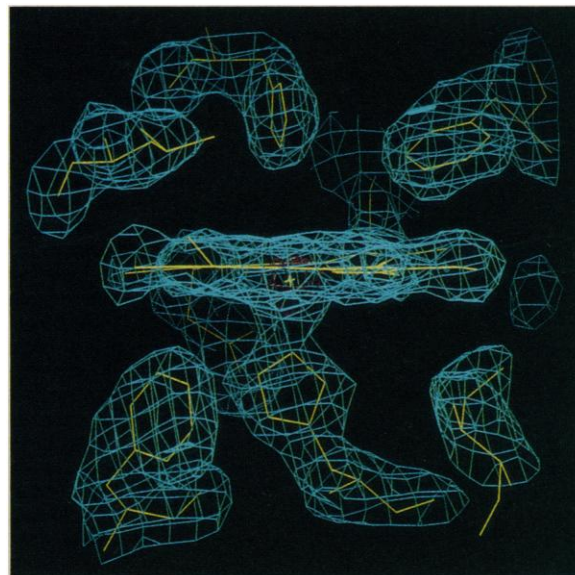
A 3.2 Å electron density map from deoxy crystals (7) was obtained by a combination of anomalous scattering and molecular replacement (8). This map clearly demonstrated the absence of any ligand at the oxygen binding site and revealed a number of striking differences in the tertiary structure of the subunits between liganded and unliganded forms. A molecular model for the deoxy structure was obtained by refitting the heme group and nine residues (in each subunit) and was used as the starting point for stereochemically restrained least-squares refine-

ment (9). The deoxy structure has now been refined to an *R* value of 0.160 at 2.4 Å resolution (Table 1 and Fig. 1). In addition, the CO-liganded structure has been improved by slightly refitting four residues, modeling the solvent slightly differently, and performing an additional 14 cycles of least-squares refinement. The *R* value decreased from 0.156 to 0.152 at 2.4 Å resolution with a slight improvement in stereochemistry.

The overall quaternary difference between the CO-liganded and deoxy states is relatively small (Fig. 2). An optimized superposition (10) of α -carbons in the individual subunits showed that the movement of one subunit relative to the second subunit upon ligand binding can be described by a screw axis rotation of 3.4° with a translation of 0.1 Å. The "E-E" region of the interface (6) acts as a pivot in the subunit rotation with the packing of Tyr⁷⁵ against Asn⁷⁹ virtually unchanged in the two structures. (Primes designate the symmetry-related subunit.) In contrast, for mammalian hemoglobins the $\alpha_1\beta_1$ dimer rotates relative to the $\alpha_2\beta_2$ dimer by 15° and translates by 0.8 Å in the transition between the unliganded and liganded states (2).

Whereas the quaternary structural changes are rather subtle, striking tertiary structural differences are evident between the two structures. The most dramatic difference in conformation between the two structures is observed for Phe⁹⁷ (Figs. 3 and 4). In the deoxy structure the phenyl group packs tightly against the heme on the proximal side. In the CO structure, the phenyl group packs tightly against the heme on the proximal side. The deoxy porphyrin iron atom lies nearly 0.5 Å out of the mean plane of the heme and 0.3 Å out of the plane

Fig. 1. Fragment difference electron density map of deoxy *Scapharca* dimeric hemoglobin structure. Contours are shown in blue (0.2 e/Å³) and red (1.0 e/Å³), bonds between atoms in yellow. The atoms for the heme, Phe⁵¹, Phe⁹⁷, His⁶⁹ (distal), His¹⁰¹ (proximal), Leu⁷³, and Ile¹⁰⁶ were not used in the calculation of phases for this map and are shown embedded in the map. Note the absence of ligand in the binding region (just above the heme plane) and the packing of Phe⁹⁷ (bottom left) against the heme.



formed by the porphyrin nitrogen atoms. This provides just enough room for the phenyl ring to pack against the heme. The CO-liganded iron atom is within 0.1 Å of the mean heme plane, and there is no longer sufficient space for the phenyl ring in the heme pocket.

Another major difference between the structures occurs with the heme atoms. As observed in mammalian hemoglobins (2), each deoxy clam heme is domed and the iron atom is displaced towards the proximal His¹⁰¹. In the CO structure, the hemes are more planar and are domed slightly in the opposite direction. Additionally, each heme group drops 0.6 Å deeper into its subunit upon ligand binding (Fig. 2), and the distance between iron atoms increases from 16.7 Å to 18.4 Å. This heme movement can be seen as a consequence of dislodging Phe⁹⁷, which acts as a wedge in the deoxy structure to push the proximal histidine and heme toward the subunit interface. The heme groups of both structures are quite directly linked across the subunit interface, but this is accomplished differently in the two cases (see Fig. 3). In the close deoxy interface, this linkage is mediated by a pair of folded propionates that are bridged by pairs of hydrogen bonds from Asn¹⁰⁰ and Asn^{100'}. These propionates pull away and are extended in the CO structure where they are bridged by a water molecule, and each is hydrogen bonded separately across the interface to Asn^{100'} and to Lys⁹⁶. The other propionate from each heme is salt bridged to Lys⁹⁶ in the deoxy but not in the CO structure.

A hydrogen bond between Nδ of the proximal His (F14) and the main chain carbonyl of residue F10 (Phe⁹⁷) appears to couple the movements of these two residues. A similar hydrogen bond is also formed in other hemoglobins, and this has been suggested to be a pathway linking the protein conformation with reactivity of the heme iron (11). In particular, the electron withdrawing character of CO and O₂ (12) should cause a net shift of electrons from the proximal His and strengthen the hydrogen bond involving the His Nδ. The small differences in geometry of this hydrogen bond between liganded and unliganded structures suggest that its role may be slight in mammalian hemoglobins (2), but it could be more important in clam dimeric hemoglobin. For the CO state, the hydrogen bond distances are 2.9 and 2.8 Å in the two subunits, whereas for the deoxy state the bond is longer (3.1 and 3.3 Å) (Fig. 4). The longer hydrogen bond in the deoxy state is necessitated by the tight packing of Phe⁹⁷ against not only the heme group but also against Ce of the proximal His. The more positively

Table 1. Crystal parameters and refinement statistics for *Scapharca* dimeric deoxy and CO-liganded crystals. Both structures are based on data with Bragg spacings between 10 and 2.4 Å; rms, root mean square, and *I*, intensity.

Parameters	Deoxy	CO
Space group	C222 ₁	C2
<i>a</i> (Å)	91.79	93.25
<i>b</i> (Å)	44.45	43.98
<i>c</i> (Å)	143.81	83.50
β (degrees)	90.0	122.03
Reflections (<i>I</i> > 2.5σ _{<i>I</i>})	10,959	10,423
Hemoglobin atoms	2,332	2,336
Solvent molecules	155	213
<i>R</i> value*	0.160	0.152
Deviations, rms		
Bond (Å)	0.014	0.013
Angle (degrees)	1.8	1.7
Noncrystallographic symmetry† (Å)	0.172	0.128

* $R = \sum ||F_o| - F_c| / \sum |F_o|$. †Noncrystallographic symmetry restraints were applied in the deoxy refinement for the first 50 cycles but were not used for the last 44 cycles. The deviations listed include all main chain atoms for the deoxy structure but only residues 10 to 146 for the CO model.

charged proximal His resulting from ligand binding would tend to strengthen and shorten the hydrogen bond. This, along with the movement of the iron and proximal His into the plane of the heme, would have the effect of expelling the Phe from the heme pocket. Conversely, the longer hydrogen bond, together with heme buckling induced by the Phe-heme interaction, may tend to decrease the affinity for oxygen in the deoxy state.

Thus, Phe⁹⁷ appears to play a major role in maintaining the deoxygenated molecule in a low-affinity state. Cooperativity requires that binding of oxygen to one subunit causes the second subunit to attain a higher affinity conformation. Since ligand binding to one subunit is probably coupled with the

expulsion of the phenyl group from the heme pocket, movements associated with this action could be crucial for communication between the hemes. One possible effect would be due to interactions of the phenyl ring in the interface and a second would result from the sinking of the heme group deeper into the subunit.

The expulsion of the Phe⁹⁷ side chain from the heme pocket into the interface disrupts a network of some 14 water molecules by pushing out at least three from the vicinity of Thr⁷², thereby changing the character of this region from hydrophilic to hydrophobic. Rearrangements must then occur that allow a close van der Waals contact to form in the CO structure between the methyl carbon of Thr⁷² and Cζ of Phe⁹⁷

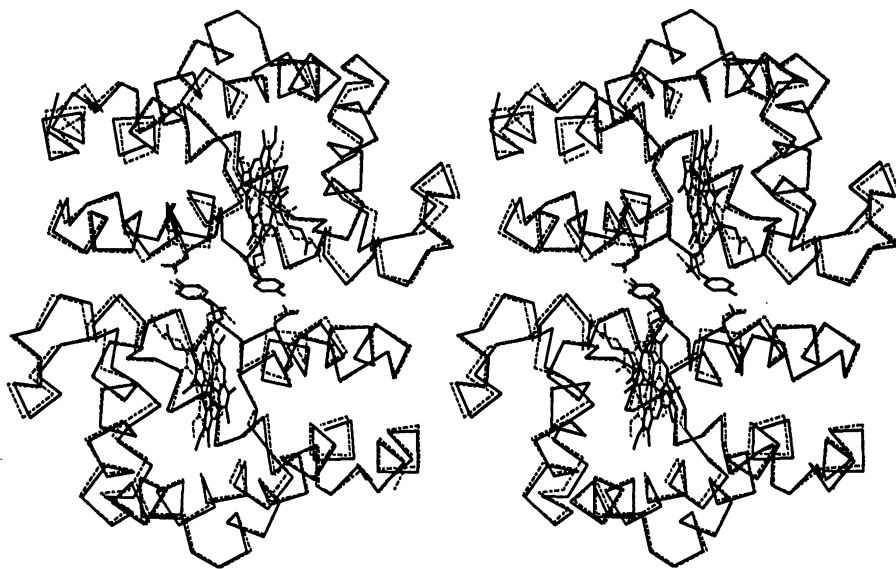


Fig. 2. Stereoplot showing superposition of deoxy (dashed lines) and CO (solid lines) dimer structures. In addition to the α-carbon plot, the hemes and side chains for residues 75 and 79 are shown for both structures. Note the slight overall rearrangement of subunits upon ligand binding, the movement of the hemes deeper into the subunit upon ligation, and the similarity of packing of Tyr⁷⁵ against Asn⁷⁹ in the E helices.

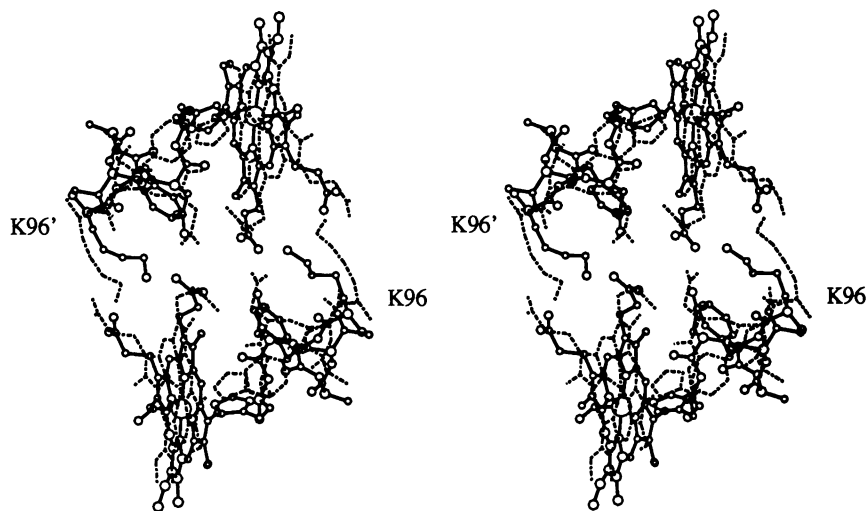


Fig. 3. Stereoplots of the last two turns of the F helix and hemes for both subunits for the deoxy (dashed lines) and CO (atom circles and dark bonds) dimer structures. The side chains for Lys^{96'} can be seen at the right and Lys^{96'} at the left side. Note how the amino groups switch from interacting with one propionate to the other propionate upon CO ligation. Next to Lys^{96'} is Phe^{97'}, whose side chain is packed against the heme and the proximal His^{101'} in the deoxy state but is extruded towards the subunit interface in CO state. The closer approach of the hemes in the deoxy state requires one set of propionates to fold over in order to avoid unacceptably close contact.

(3.2 and 3.5 Å). Movements of the main chain atoms of Thr^{72'} and Leu^{73'} (relative to the rest of the subunit) are about 0.3 Å and the Leu^{73'} side chain moves by up to 1 Å. Interestingly, Leu^{73'} packs against the heme on the distal (ligand binding) side directly opposite Phe^{97'} in the deoxy structure, and the Leu^{73'} side chain moves in the direction of the heme plane as the heme in the CO structure becomes more planar and Phe^{97'} leaves the proximal side of the heme pocket. It is tempting to speculate that Leu^{73'} (in an unliganded subunit) could play a role in the cooperative oxygen binding by being pushed toward the heme after Thr^{72'} and Phe^{97'} (upon ligation of the first subunit) move closer together and thus help to eject the phenyl ring of Phe^{97'} and promote ligation. However, an alternative explanation based on Leu^{73'} being pulled in by the heme group after Phe^{97'} leaves the heme pocket cannot be discounted.

The direct involvement of heme propionates in the subunit interface suggests that the sinking of the heme into the subunit upon ligation could be another reasonable trigger for heme-heme communication. This movement and the unbuckling of the heme would weaken the salt bridge present in the deoxy structure between one of the heme propionates and the amino group of Lys^{96'} by increasing the distance 0.3 to 0.5 Å. Additionally, the other propionate will be brought into a better position to interact with Lys^{96'} and its negative charge may pull on the positively charged amino group. A geometrically satisfactory salt bridge requires rearrangements of main chain atoms

as well as side chain atoms. Movements of main chain atoms of Lys^{96'} and Phe^{97'} of about 1 Å towards the heme after ligand binding are observed and require the extrusion of the phenyl ring from the heme pocket (see Fig. 2). In this way, pulling Lys^{96'} may encourage ligation of the second subunit.

The packing of Phe^{97'} at the interface in CO hemoglobin but not deoxy hemoglobin suggests a possible fundamental difference in the linkage between assembly and ligation in clam versus human hemoglobin. In human hemoglobin, cooperativity results primarily from a ligand-induced stepwise reduction of "quaternary constraints" imposed by the assemblage (13). This has two measurable effects: (i) isolated chains bind oxygen with higher affinity than does the native tetramer; and (ii) the unliganded assemblage is more tightly associated than the liganded assemblage. However, once three ligands have bound to human hemoglobin, the fourth is bound with higher affinity than in isolated chains or αβ dimers (14). Consequently, triliganded human hemoglobin is less tightly associated than fully liganded hemoglobin. This increase in affinity over isolated chains has been termed "quaternary enhancement" and its magnitude is about one-fourth the magnitude of "quaternary constraint" in the unliganded tetramer (14). In clam hemoglobin "quaternary enhancement" could play the primary role in cooperativity. An isolated subunit would have to expel Phe^{97'} toward bulk solvent upon oxygenation, whereas in the dimer a somewhat more hydrophobic surface is available. This

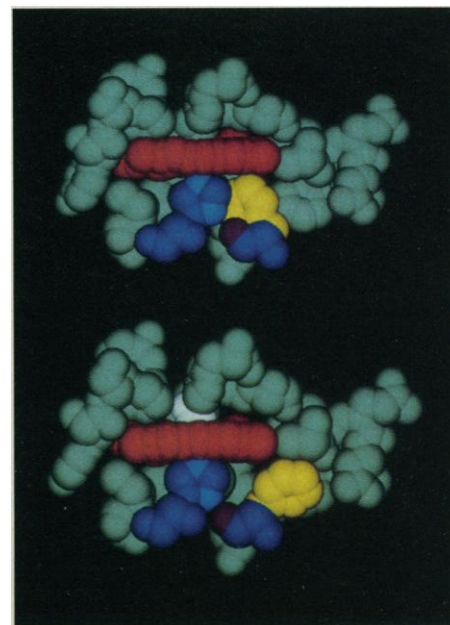


Fig. 4. Raster display showing the ligand-induced movement of Phe^{97'} between the deoxy (**top**) and CO (**bottom**) structures. The phenyl ring is shown in yellow, the heme is shown in red, and the CO ligand is shown in white. Note that upon expulsion of the phenyl ring from the heme pocket, the hydrogen bond between the carbonyl oxygen (purple) of Phe^{97'} and the Nδ (light blue) of the proximal His^{101'} shortens.

suggests that isolated subunits may bind oxygen with lower affinity than the dimer. Then, because of the linkage between ligand binding and subunit association, a liganded dimer would be more tightly associated than the unliganded dimer. Thus the dimeric assemblage may enhance rather than constrain oxygen affinity, and ligand binding may tighten rather than loosen the association of subunits. This hypothesis remains to be tested by thermodynamic experiments.

Although these structures are well refined at 2.4 Å resolution, the root-mean-square coordinate error in each structure could be as high as 0.25 Å and a hint of some coordinate error is evident in the differences in distances seen in the two subunits. While the major structural transitions involve large motions, some aspects involve changes measured in fractions of an angstrom. Thus, it is essential that the molecular models have the greatest possible accuracy. Diffraction from both crystal forms is apparent to higher angles ($d_{\min} < 1.5$ Å for each) and higher resolution structures should better define changes that occur upon ligand binding.

REFERENCES AND NOTES

1. H. K. Schachman, *J. Biol. Chem.* **263**, 18583 (1988); S. E. V. Phillips *et al.*, *Nature* **341**, 711 (1989).

- M. F. Perutz, G. Fermi, B. Luisi, B. Shaanan, R. C. Liddington, *Acc. Chem. Res.* **20**, 309 (1987).
- S. Ohnoki, Y. Mitomi, R. Hata, K. Satake, J. *Biochem.* **73**, 717 (1973); H. Furuta, M. Ohe, A. Kajita, *ibid.* **82**, 1723 (1977); P. F. Como and E. O. P. Thompson, *Aust. J. Biol. Sci.* **33**, 643 (1980); E. Chiancone, P. Vecchini, D. Verzili, F. Ascoli, E. Antonini, *J. Mol. Biol.* **152**, 577 (1981); R. C. San George and R. L. Nagel, *J. Biol. Chem.* **260**, 4331 (1985); T. A. Borgese, J. P. Harrington, D. Hoffman, R. C. San George, R. L. Nagel, *Comp. Biochem. Physiol.* **86B**, 155 (1987).
- M. Ikeda-Saito *et al.*, *J. Mol. Biol.* **170**, 1009 (1983).
- W. E. Royer, Jr., W. E. Love, F. F. Fenderson, *Nature* **316**, 277 (1985).
- W. E. Royer, Jr., W. A. Hendrickson, E. Chiancone, *J. Biol. Chem.* **264**, 21052 (1989).
- Deoxy crystals of the *Scapharca* dimer were grown from solutions of 18 mg/ml hemoglobin in 1.7 M phosphate buffer at pH 8.5 in a Bactron I anaerobic chamber (Anaerobe Systems, Santa Clara, CA). Single, diffraction-quality crystals were only obtained by using microseeding techniques [P. M. D. Fitzgerald and N. B. Madsen, *J. Cryst. Growth* **76**, 600 (1986)]. Spectra from dissolved crystals verified the deoxygenated state of the hemoglobin in these crystals. Both the deoxy and carbon monoxide crystals contain a complete dimer per asymmetric unit. As shown in Table 1, the deoxy crystals, although not isomorphous to the carbon monoxide crystals, are clearly related. In particular, the a and b unit cell axial lengths are nearly the same in both crystal forms and the deoxy c-axis length is twice $1/c^*$ of the liganded crystals. Thus, the packing of molecules in the ab plane would be similar in both crystal forms. This reduces lattice effects in comparisons between the CO and deoxy crystals. Those lattice contacts that are different have minimal effects on the dimeric interface.
- Diffraction data were collected on an AFC5R diffractometer (Molecular Structure Corporation) from deoxy crystals that had been mounted in the anaerobic chamber in thin-walled glass capillaries and sealed with mercury and DeKhotinsky cement (Thomas Scientific). The data included Friedel pairs from two crystals for reflections corresponding to Bragg spacings greater than 3.2 Å and from a third crystal used to obtain the unique data between 3.2 and 2.4 Å. An anomalous difference Patterson map [M. G. Rossmann, *Acta Crystallogr.* **14**, 383 (1961)] clearly revealed the iron positions and confirmed the approximate packing of molecules expected from comparisons with the CO structure. The orientation and position of the subunits were then refined independently against the diffraction data to an R value of 0.34 at 4.0 Å resolution. This molecular replacement model was used to break phase ambiguities derived from the anomalous scattering experiment. These models resolved anomalous phases [J. L. Smith and W. A. Hendrickson, in *Computational Crystallography*, D. Sayre, Ed. (Oxford Univ. Press, New York, 1982), pp. 209–222; S. Sheriff, W. A. Hendrickson, J. L. Smith, *J. Mol. Biol.* **197**, 273 (1987)] were used to calculate a map at 3.2 Å resolution that was further improved by 13 cycles of symmetry averaging.
- W. A. Hendrickson and J. H. Konner, in *Computing in Crystallography*, R. Diamond, S. Ramaseshan, K. Venkatesan, Eds. (Indian Academy of Sciences, Bangalore, 1980), pp. 13.01–13.23; W. A. Hendrickson, *Methods Enzymol.* **115**, 252 (1985).
- W. A. Hendrickson, *Acta Crystallogr.* **A35**, 158 (1979).
- J. S. Valentine, R. P. Sheridan, L. C. Allen, P. C. Kahn, *Proc. Natl. Acad. Sci. U.S.A.* **76**, 1009 (1979); P. Stein, M. Mitchell, T. G. Spiro, *J. Am. Chem. Soc.* **102**, 7795 (1980).
- W. S. Caughey, C. H. Barlow, J. C. Maxwell, J. A. Volpe, W. J. Wallace, *Ann. N.Y. Acad. Sci.* **244**, 1 (1975); C. H. Barlow, J. C. Maxwell, W. J. Wallace, W. S. Caughey, *Biochem. Biophys. Res. Commun.* **55**, 91 (1973).
- G. K. Ackers, *Biophys. J.* **32**, 331 (1980).
- F. C. Mills and G. K. Ackers, *Proc. Natl. Acad. Sci. U.S.A.* **76**, 273 (1979).
- We thank F. Smith for discussions about anaerobic crystallizations and suggesting the use of the Bactron I anaerobic chamber and S. Hubbard and H.-E. Aronson for computer programs. The atomic coordinates and diffraction data are being deposited in the Brookhaven Protein Data Bank. This work was supported in part by a grant for the National Science Foundation (DMB 87-17570).

1 March 1990; accepted 5 June 1990

Molecular Structure of Charybdotoxin, a Pore-Directed Inhibitor of Potassium Ion Channels

WALTER MASSEFSKI, JR., ALFRED G. REDFIELD, DENNIS R. HARE, CHRISTOPHER MILLER

The three-dimensional structure of charybdotoxin, a high-affinity peptide blocker of several potassium ion channels, was determined by two-dimensional nuclear magnetic resonance (2-D NMR) spectroscopy. Unambiguous NMR assignments of backbone and side chain hydrogens were made for all 37 amino acids. The structure was determined by distance geometry and refined by nuclear Overhauser and exchange spectroscopy back calculation. The peptide is built on a foundation of three antiparallel β strands to which other parts of the sequence are attached by three disulfide bridges. The overall shape is roughly ellipsoidal, with axes of approximately 2.5 and 1.5 nanometers. Nine of the ten charged groups are located on one side of the ellipsoid, with seven of the eight positive residues lying in a stripe 2.5 nanometers in length. The other side displays three hydrophobic residues projecting prominently into aqueous solution. The structure rationalizes several mechanistic features of charybdotoxin block of the high-conductance Ca^{2+} -activated K^+ channel.

AMONG THE NEUROTOXINS PRESENT in the venoms of buthid scorpions is a family of peptides that specifically inhibit certain K^+ -specific ion channels found in electrically excitable membranes (1, 2). Of these peptides, charybdotoxin (CTX) is the best studied at the mechanistic and

biochemical levels (3, 4). It is known (5) that CTX inhibits its K^+ channel target by binding to the externally facing ion entryway and physically blocking the permeation of K^+ ions. Because of this simple mode of action, CTX has proven valuable as a probe of the molecular nature of K^+ channels, including the size of the external channel "mouth" and the disposition of charges on the channel protein surface (5). Our ability to use CTX in this way would be greatly enhanced by a knowledge of the peptide's 3-D structure. Since the toxin is only a minor component of venom proteins in even the richest known source, it is not feasible at present to under-

take crystallization studies that would lead to structure determination by x-ray crystallography. However, the peptide's small size (37-amino acid residues), known primary sequence, and conformational rigidity resulting from its three disulfide bonds make it an appropriate target for attack by 2-D NMR methods. In this report, we describe the use of this technique to determine the solution structure of CTX.

The 1-D ^1H NMR spectra of a sample of CTX at pH 4.0 in both D_2O and H_2O (Fig. 1A) demonstrate that the sample produces high-quality peaks suitable for 2-D NMR procedures (6). A homonuclear Hartmann-Hahn transfer (HOHAHA) experiment (Fig. 1B), which yields a map of through-bond couplings, illustrates the well-resolved cross peaks in the $\text{H}\alpha$ - $\text{H}\beta$ region. Assignment of individual protons to the resonance lines was done in two stages (7). First, side chains were assigned as far as possible from the scalar coupling patterns of correlation spectroscopy (COSY), HOHAHA, and double-quantum experiments. This process was straightforward for aromatic residues, since each (Phe, Trp, Tyr, and His) occurs only once in CTX. The methyl-containing residues were easily divided into amino acid types, since only one Leu, two Val, and four Thr residues are present in CTX. Glycine-26 was identified by a single $\text{NH-H}\alpha$ remote peak in the double-quantum experiment. Serines were identified from the rest of $\alpha\beta_2$ spin systems by their unusually downfield β protons (Fig. 1B). The unique glutamate

W. Massefski, Jr., Graduate Department of Biochemistry, Brandeis University, Waltham, MA 02254.
A. G. Redfield, Graduate Department of Biochemistry and Physics, Brandeis University, Waltham, MA 02254.
D. R. Hare, Hare Research, Inc., Woodinville, WA 98072.

C. Miller, Howard Hughes Medical Institute, Graduate Department of Biochemistry, Brandeis University, Waltham, MA 02254.